Direct-Potential-Fit for $Li_2(A\,^1\Sigma_u^+)$ using a Potential Form that Incorporates the Transition from Hund's Case (a) to Hund's Case (c) Coupling

Robert J. Le Roy,[a,b] Amanda J. Ross,[c] and Colan Linton[b,d]

[a] Guelph-Waterloo Centre for Graduate Work in Chemistry and Biochemistry, University of Waterloo, Waterloo, Ontario, Canada

[b] Université Lyon 1; CNRS; LASIM UMR 5579, 43 Bd du 11 novembre 1918, F-69622 Villeurbanne, France

[d] Physics Department, University of New Brunswick, Fredericton, NB E3B 5A3, Canada

[b] Research supported by the Natural Sciences and Engineering Research Council of Canada

Spectroscopists' traditional approach for diatomics

- Represent level energies as power series in $(v+\frac{1}{2})$ and $[J(J+1)]$:

$$E(v,J) \;=\; T_e \;+\; \sum_{m=0}\sum_{l=0}{}' \; Y_{l,m}\,(v+\tfrac{1}{2})^l\,[J(J+1)]^m$$

- Use the semiclassical "RKR" method to determine a point-wise potential

$$r_2(G_v) \;-\; r_1(G_v) \;=\; 2\sqrt{\tfrac{\hbar^2}{2\mu}}\int_{v_{min}}^{v}\frac{1}{[G_v-G_{v'}]^{1/2}}\,dv'$$

$$\frac{1}{r_1(G_v)} \;-\; \frac{1}{r_2(G_v)} \;=\; 2\sqrt{\tfrac{2\mu}{\hbar^2}}\int_{v_{min}}^{v}\frac{B_{v'}}{[G_v-G_{v'}]^{1/2}}\,dv'$$

Yields a very precisely defined and smooth ($\approx$ to machine precision) potential!

Problems:

- *Very limited extrapolation ability.*
- Since the RKR method is based on the first-order semiclassical approximation, it *has limited accuracy* for small-reduced-mass systems.
- A potential defined as an irregular mesh of points, with distances specified to many significant-digit, *is inconvenient to work with!*

Direct Potential Fits

{*Applied to 3-D Van der Waals molecules since 1974, and to diatomics since* $\sim$ 1990 }

- Simulate level energies as numerically (or algebraically) determined eigenvalues of some parameterized analytic potential energy function $V(r;\{p_j\})$.
- Partial derivatives of observables w.r.t. parameters p_j required for fitting are generated readily by the Hellmann-Feynmann theorem:

$$\frac{\partial E(v,J)}{\partial p_j} = \left\langle \psi_{v,J} \left| \frac{\partial V(r;\{p_j\})}{\partial p_j} \right| \psi_{v,J} \right\rangle$$

- Compare predicted transition energies with experiment, and optimize the potential parameters via an iterative least-squares fit.

Advantages

- allows realistic predictions in 'extrapolation' region outside the data range, and hence also allows prediction of collisional properties
- yields full quantum mechanical accuracy
- readily takes account of Born-Oppenheimer breakdown (BOB), Λ-doubling, and/or $^2\Sigma$ splittings, in terms of radial strength functions

Challenge ... to develop analytic potential function forms which

* are flexible enough to fully represent all available (high-resolution) data
* are robust and 'well behaved' (no spurious behaviour in extrapolation regions)
* incorporate appropriate physical constraints and limiting behaviour

Three Types of Potentials

1. Polynomial expansion $V(r) = c_0\,\xi^2\left(1 + \sum_{i=1} c_i\,\xi^i\right)$ in variable:

- Dunham $\xi_{\rm D} = \dfrac{r - r_e}{r_e}$
- Ogilvie-Tipping $\xi_{\rm OT} = \dfrac{r - r_e}{r + r_e}$
- Tiemann *et al.* $\xi_{\rm T} = \dfrac{r - r_e}{r + b\,r_e}$
- Simons-Parr-Finlan $\xi_{\rm SPF} = \dfrac{r - r_e}{r}$
- Šurkus ('GPEF') $\xi_{\rm Sur} = \dfrac{r^p - {r_e}^p}{a_S\,r^p + b_S\,{r_e}^p}$

Problems associated with such polynomial potentials .....

- good fits require a relatively large numbers of terms
- polynomials generally behave badly outside the 'data region'
- realistic inverse-power long-range behaviour can only be be imposed by attaching an inverse-power function at some *ad hoc* chosen distance $r_{\rm out}$

2. Spline-Point-wise Potentials

- potential in 'data region' is cubic spline function on a selected radial mesh: potential-fit parameters are energies of those spline points
- attach an inverse-power long-range tail at some chosen outer bound $r_{\rm out}$

3. Coxon-type Global Analytic Potentials based on Morse Form

$$V_{\rm CGF}(r) \;=\; \mathfrak{D}_e \left[1 - Q(r)\; e^{-\beta(r)\,(r-r_e)} \right]^2$$

with $Q(r)$ defined such that $Q(r_e) = 1$,

- algebraic structure defines gross potential shape
- only modest variation of $\beta(r)$ provides precise representation of full potential
- early work used $Q(r) \equiv 1$ and $\beta(r) = \sum_{i=0} \beta_i\; (r - r_e)^i$

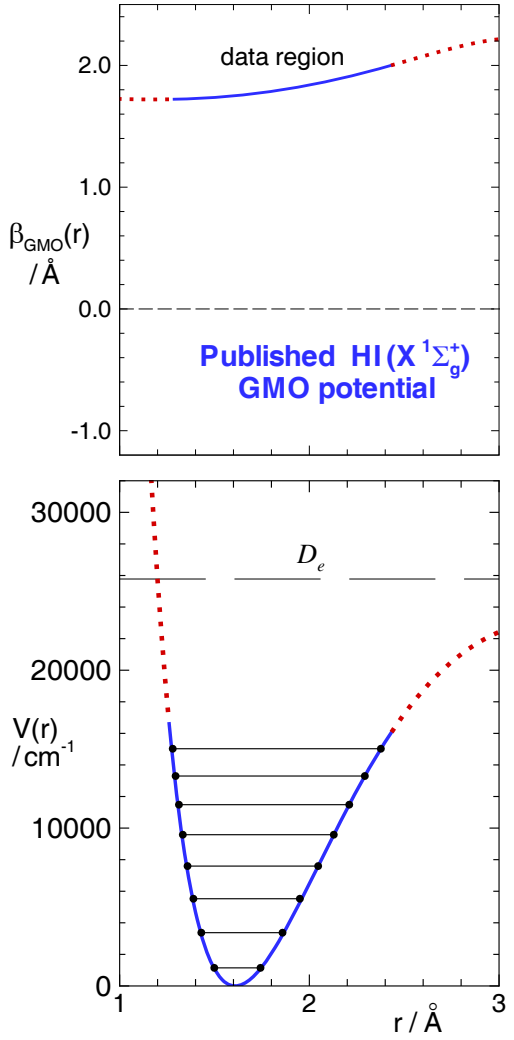

2. Spline-Pointwise Potentials

- potential in 'data region' is cubic spline function on a selected radial mesh: potential-fit parameters are energies of those spline points
- attach an inverse-power long-range tail at some chosen outer bound $r_{\rm out}$

3. Coxon-type Global Analytic Potentials based on Morse Form

$$V_{\rm CGF}(r) \;=\; \mathfrak{D}_e \left[1 - Q(r)\; e^{-\beta(r)\,(r-r_e)} \right]^2$$

with $Q(r)$ defined such that $Q(r_e) = 1$,

- algebraic structure defines gross potential shape
- only modest variation of $\beta(r)$ provides precise representation of full potential
- early work used $Q(r) \equiv 1$ and $\beta(r) = \sum_{i=0} \beta_i\; (r - r_e)^i$

but it sometimes gave problems . . .

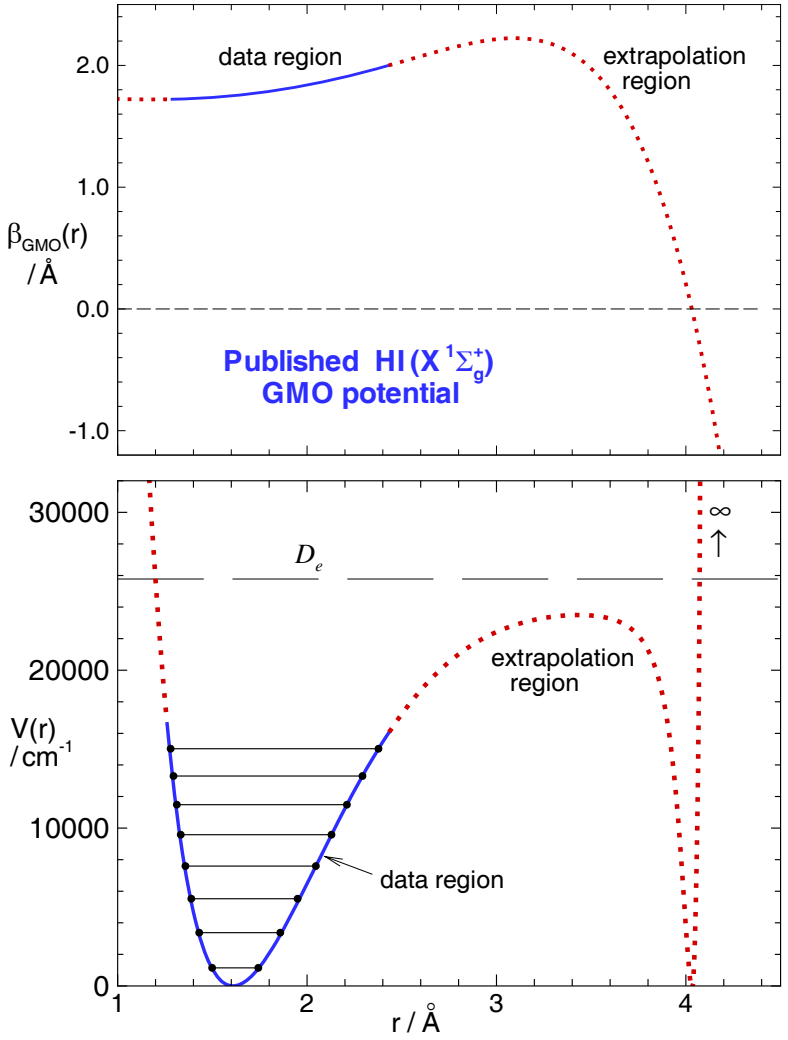

However . . . . . .

- replacing the simple polynomial for exponent coefficient $\beta(r)$ by an expansion in a radial variable which is well-behaved on the whole interval $y_p(r) = \dfrac{r^p - {r_e}^p}{r^p + {r_e}^p}$ suppresses unphysical extrapolation behaviour !
- defining $Q(r)$ appropriately yields a potential with proper inverse-power long-range behaviour

Morse/Long-Range (MLR) Potential

If we define $u_{\rm LR}(r) = \dfrac{C_{m_1}}{r^{m_1}} + \dfrac{C_{m_2}}{r^{m_2}} + \ldots$ we can write

$$V_{\rm MLR}(r) = \mathfrak{D}_e \left\{ 1 - \left(\frac{u_{\rm LR}(r)}{u_{\rm LR}(r_e)} \right) e^{-\phi(r)\, y_p(r)} \right\}^2$$

$$\xrightarrow{r \gg r_e} \mathfrak{D}_e - \left[\frac{2\,\mathfrak{D}_e\, e^{-\phi_\infty}}{u_{\rm LR}(r_e)} \right] u_{\rm LR}(r) = \mathfrak{D}_e - \frac{C_{m_1}}{r^{m_1}} - \frac{C_{m_2}}{r^{m_2}} - \ldots$$

in which $\phi_\infty \equiv \phi(r=\infty) = \ln\{2\,\mathfrak{D}_e / u_{\rm LR}(r_e)\}$

and $\phi(r) = \phi_{\rm MLR}(r) = \phi_\infty\, y_p(r) + [1 - y_p(r)] \sum_{i=0}^{N} \phi_i\, y_p(r)^i$

This model has recently been applied to analyses of data for $\mathrm{N_2}(X\,{}^1\Sigma_g^+)$, for $\mathrm{KLi}(a\,{}^3\Sigma^+)$ and for $\mathrm{Ca_2}(X\,{}^1\Sigma_g^+)$.

Tiemann polynomial	
$\mathfrak{D}_e$	1102.074
r_e	
C_6	1.0030×10^{7}
C_8	3.87×10^{8}
C_{10}	4.41×10^{9}
b	-0.5929
a_0	0.00043
a_1	-2.57153863528197002
a_2	$3.79611687289805877\times10^{3}$
a_3	$3.82947943867555637\times10^{2}$
a_4	$-2.74470356912936631\times10^{3}$
a_5	$-3.23378807398046092\times10^{3}$
a_6	$3.70205119299758223\times10^{2}$
a_7	$6.35318559107446436\times10^{3}$
a_8	$-7.39783474312859562\times10^{3}$
a_9	$-1.90759867971015337\times10^{4}$
a_{10}	$5.41779135173975228\times10^{4}$
a_{11}	$4.40527349765557083\times10^{4}$
a_{12}	$-1.55406021572582802\times10^{5}$
a_{13}	$-8.35826911941128783\times10^{4}$
a_{14}	$2.13873243831604603\times10^{5}$
a_{15}	$1.56022970979522303\times10^{5}$
a_{16}	$-1.56329579530082468\times10^{5}$
a_{17}	$-1.46822446075956163\times10^{5}$
a_{18}	$2.74480910039127666\times10^{4}$
a_{19}	$7.11882274192053592\times10^{4}$
a_{20}	$-7.63044568335207146\times10^{2}$
r_m	4.277277 Å
$r_{\rm out}$	9.5

Spline point-wise potential			
$\mathfrak{D}_e$	1102.060		
C_6	1.0023×10^{7}		
C_8	3.808×10^{8}		
C_{10}	$5.06\ \times10^{9}$		
r/Å	U/cm^{-1}	r/Å	U/cm^{-1}
3.096980	9246.6895	5.678571	636.3741
3.188725	6566.7325	5.809524	684.9589
3.280470	4525.7282	5.940476	728.9235
3.372215	3090.9557	6.071429	768.5976
3.463960	2134.2175	6.202381	804.2551
3.555705	1475.2425	6.333333	836.2419
3.647450	1004.5043	6.464286	864.8746
3.739195	661.4123	6.595238	890.4666
3.830940	410.6117	6.726191	913.2923
3.922685	234.0001	6.857143	933.6417
4.014430	116.0996	6.988095	951.7718
4.106174	44.5437	7.119048	967.8632
4.197920	8.6885	7.250000	982.2159
4.289664	0.1760	7.500000	1005.2497
4.381409	11.9571	7.750000	1023.6698
4.500000	48.5948	8.000000	1038.3262
4.630952	106.9081	8.358974	1054.3861
4.761905	175.7311	8.717949	1066.0579
4.892857	248.8199	9.076923	1074.5969
5.023809	322.3873	9.435897	1080.8961
5.154762	393.7222	9.794872	1085.5974
5.285714	461.4555	10.303419	1090.2990
5.416667	524.6311	10.811966	1093.5160
5.547619	582.9870	11.611111	1096.6870

$\mathbf{MLR_5(4,11)}$	
$\mathfrak{D}_e$	1102.076
r_e	4.27781
C_6	1.032×10^{7}
C_8	3.096×10^{8}
β_0	-1.074136
β_1	0.0232
β_2	-0.42734
β_3	-0.1602
β_4	-0.3443
β_5	-8.228
β_6	72.177
β_7	-291.79
β_8	639.5
β_9	-797.5
β_{10}	533.
β_{11}	$-150.$

Behaviour of MLR potentials outside the 'data region'

e.g., consider $N_2(X\,^1\Sigma_g^+)$

We can write the overall potential as

$$V(r) = \mathfrak{D} - \frac{C_6^{\rm eff}(r)}{r^6}$$

Since at long range

$$V(r) \simeq \mathfrak{D} - \frac{C_6}{r^6} - \frac{C_8}{r^8} - \ldots$$

then

$$C_6^{\rm eff}(r) \equiv r^6\,[\mathfrak{D} - V(r)]$$

$$\stackrel{r\to\infty}{\longrightarrow} C_6 + \frac{C_8}{r^2} + \ldots$$

Criterion for the best model!

Hence, a plot of $C_6^{\rm eff}(r)$ vs. $1/r^2$

should approach

- an intercept of $C_6^{\rm theory}$
- with a slope of $C_8^{\rm theory}$

from above!

Behaviour of MLR potentials outside the 'data region'

e.g., consider $N_2(X\,^1\Sigma_g^+)$

We can write the overall potential as

$$V(r) = \mathfrak{D} - \frac{C_6^{\rm eff}(r)}{r^6}$$

Since at long range

$$V(r) \simeq \mathfrak{D} - \frac{C_6}{r^6} - \frac{C_8}{r^8} - \ldots$$

then

$$C_6^{\rm eff}(r) \equiv r^6\,[\mathfrak{D} - V(r)] \xrightarrow{r\to\infty} C_6 + \frac{C_8}{r^2} + \ldots$$

Criterion for the best model!

Hence, a plot of $C_6^{\rm eff}(r)$ vs. $1/r^2$ should approach

- an intercept of $C_6^{\rm theory}$
- with a slope of $C_8^{\rm theory}$

from above!

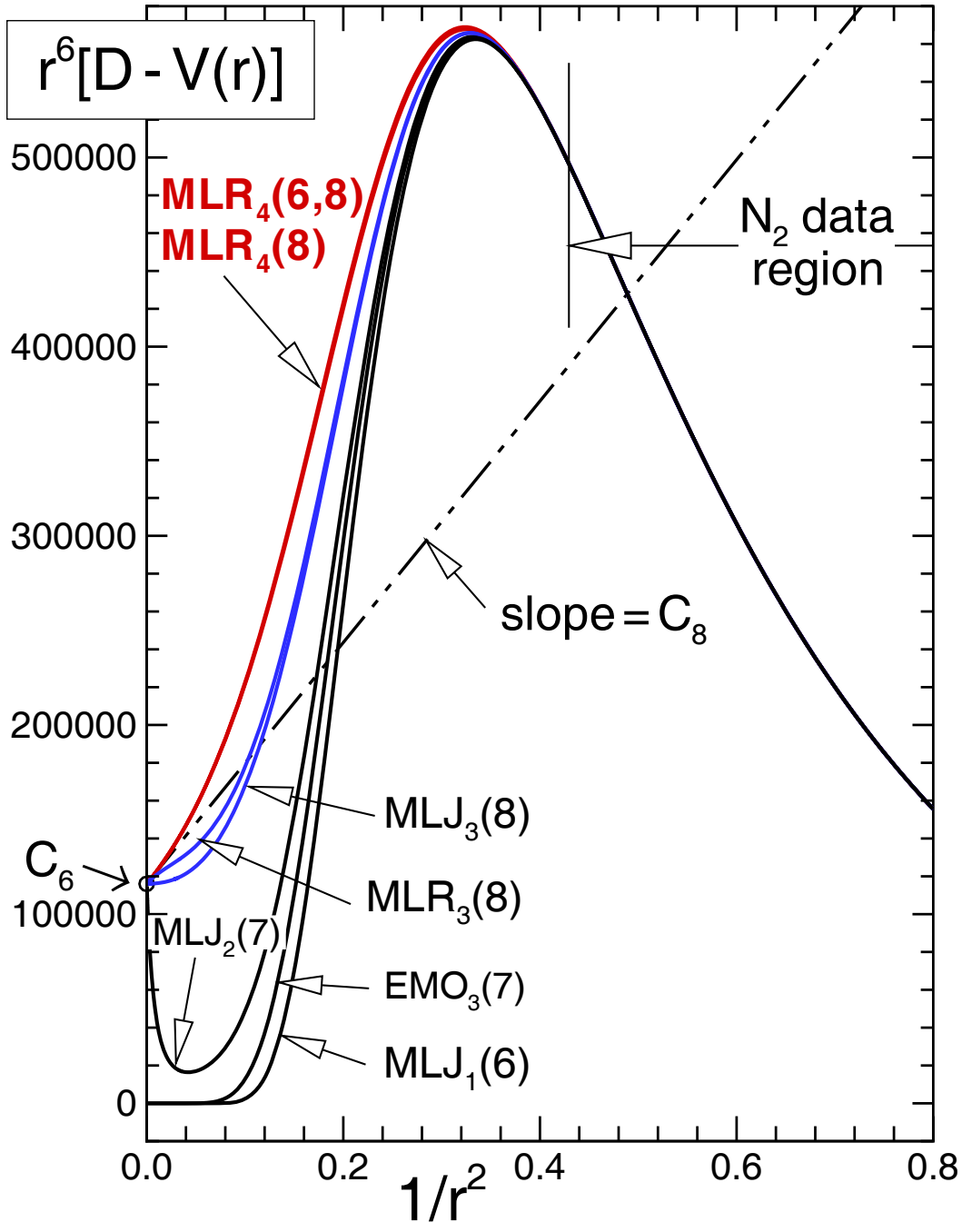

Consider the $A\,(^1\Sigma_u^+)$ *state of* Li_2

- FT absorption & emission, laser excitation & PAS data span 99.9965% of well: highest observed levels bound by $\sim 0.36\ \mathrm{cm}^{-1}$
- extensive data for both $^{7,7}\mathrm{Li}_2$ and $^{6,6}\mathrm{Li}_2$
- long-range potential has form $V(r) \simeq \mathfrak{D} - \dfrac{C_3}{r^3} - \dfrac{C_6}{r^6} - \dfrac{C_8}{r^8} - \ldots$ and the C_m coefficients are known from theory.
- *Melville & Coxon* [JMS **235**, 235 (2006)] determined an analytic MLR-type potential with *only onee* constrained long-range term (C_3/r^3), which represents all data up to $2.6\ \mathrm{cm}^{-1}$ from dissociation.

What's the problem ??

- their potential cannot accurately represent data for highest observed levels
- the asymptote of their potential function lies between the two physical asymptotes for $\mathrm{Li}(^2S) + \mathrm{Li}(^2P_{1/2})$ and $\mathrm{Li}(^2S) + \mathrm{Li}(^2P_{3/2})$

What causes this problem ??

The small ($0.3353\ \mathrm{cm}^{-1}$) spin-orbit splitting between $\mathrm{Li}(^2P_{1/2})$ and $\mathrm{Li}(^2P_{3/2})$ asymptotes enhances mixing between the $A(^1\Sigma_u^+)$ state correlating with the lower asymptote and the $b(^3\Pi_u)$ state correlating with the upper asymptote.

- at very large r, Hund's case (c) coupling is appropriate
- at moderate distances r, Hund's case (a) coupling is appropriate
- *the long-range coefficients differ for these two cases!*
- Melville-Coxon analysis considered only data in the "Hund's case (a) domain", and their potential form cannot incorporate the distance-dependent variation of the C_m coefficients from one case to the other

What's the solution ??

The Solution !!

1. M. Aubert-Frécon and co-workers showed that in the long-range region where this coupling becomes important, the overall interaction energy associated with the $0_u^+(^1\Sigma)$ and $0_u^+(^3\Pi)$ states is given by the 2×2 matrix

$$\begin{pmatrix} -\sum_n \frac{C_n(^1\Sigma_u^+) + 2\,C_n(^3\Pi_u)}{3r^n} & \frac{\sqrt{2}}{3}\sum_n \frac{C_n(^1\Sigma_u^+) - C_n(^3\Pi_u)}{3r^n} \\ \frac{\sqrt{2}}{3}\sum_n \frac{C_n(^1\Sigma_u^+) - C_n(^3\Pi_u)}{3r^n} & \Delta E_{\rm so} - \sum_n \frac{2\,C_n(^1\Sigma_u^+) - C_n(^3\Pi_u)}{3r^n} \end{pmatrix}$$

where $C_n(^1\Sigma_u^+)$ and where $C_n(^3\Pi^+)$ are the potential function coefficients in the "Hund's case (a) domain":

$$C_3(^1\Sigma_u^+) = \frac{2\,M^2}{3} \qquad C_6(^1\Sigma_u^+) = \frac{20\,R_{0,1} + 22\,R_{1,2}}{45}$$

$$C_3(^3\Pi_u) = \frac{M^2}{3} \qquad C_6(^3\Pi_u) = \frac{5\,R_{0,1} + 19\,R_{1,2}}{45}$$

- $M^2 = |\langle 2s|q_{\rm el}|2p\rangle|^2$ is the squared atomic dipole $2p \to 2s$ matrix element
- $R_{0,1}$ and $R_{1,2}$ are atomic matrix elements defining the leading contribution to the dispersion energy.
- and the overall inverse-power coefficients in the diagonal terms are the coefficients in the limiting "Hund's case (c)" domain.

2. Analytic diagonalization of this 2×2 matrix gives attractive effective adiabatic long-range potentials for the two state which approach the correct limits!

$$u_{\rm LR} \;=\; -\,\frac{\Delta E_{\rm so}}{2} \;+\; \frac{M^2}{2\,r^3} \;+\; \frac{[50\,R_{0,1}+82\,R_{1,2}]}{180\,r^6} \;\pm\frac{1}{2}\left\{\left(\frac{M^2}{9\,r^3}+\frac{[5\,R_{0,1}+R_{1,2}]}{45\,r^6}\;-\;\Delta E_{\rm so}\right)^2 + \frac{8}{9}\left(\frac{M^2}{3\,r^3}\;+\;\frac{[5\,R_{0,1}+R_{1,2}]}{15\,r^6}\right)^2\right\}^{1/2}$$

3. Using this expression in the standard definition of the MLR potential

$$V_{\rm MLR}(r) \;=\; \mathfrak{D}_e\left\{\,1\;-\;\left(\frac{u_{\rm LR}(r)}{u_{\rm LR}(r_e)}\right)e^{-\phi(r)\,y_p(r)}\,\right\}^2$$

gives a global analytic potential which incorporates the transformation from Hund's case (a) to Hund's case (c) with increasing r.

Parameters defining this potential are: $\mathfrak{D}_e$, r_e, M^2, $R_{0,1}$, $R_{2,1}$ and the ϕ_i expansion coefficients defining the exponent factor $\phi(r)$.

Results for $A(^1\Sigma_u^+)$ state Li_2

Analysis incomplete . . . but . . .

- good fit for $^{7,7}Li_2$ data up to $v = 92$
  [$(\mathfrak{D} - E_{v=92}) = 0.84$ cm^{-1}]
- 'limiting behaviour' plot extrapolates to $C_3^{case(a)}$ and approaches limiting slope $C_6^{case(a)}$ from above.

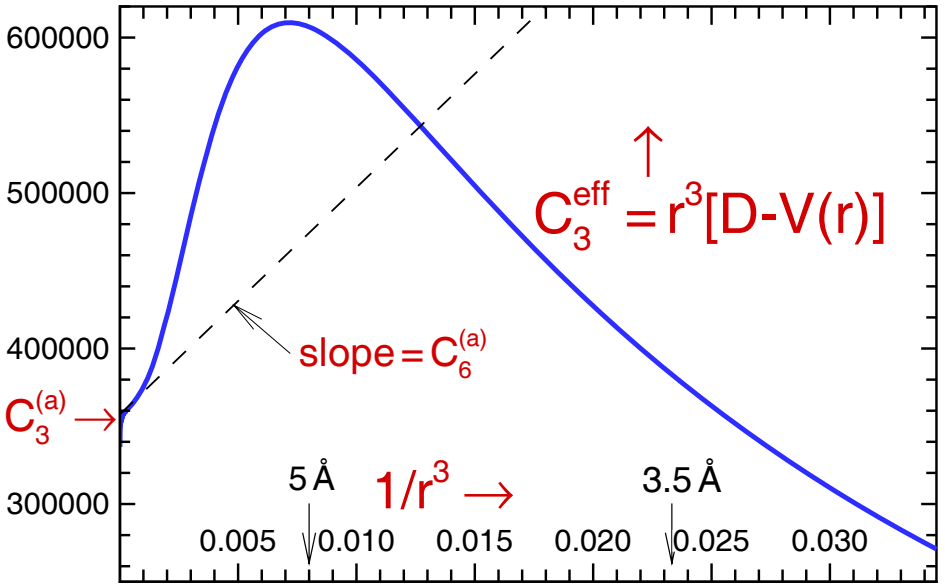

Results for $A(^1\Sigma_u^+)$ *state* Li_2

Analysis incomplete . . . but . . .

- good fit for $^{7,7}Li_2$ data up to $v = 92$
  [$(\mathfrak{D} - E_{v=92}) = 0.84\ \mathrm{cm}^{-1}$]
- 'limiting behaviour' plot extrapolates to $C_3^{case(a)}$ and approaches limiting slope $C_6^{case(a)}$ from above.
- *However . . .* expanding the scale in the large–r region shows a change of character !

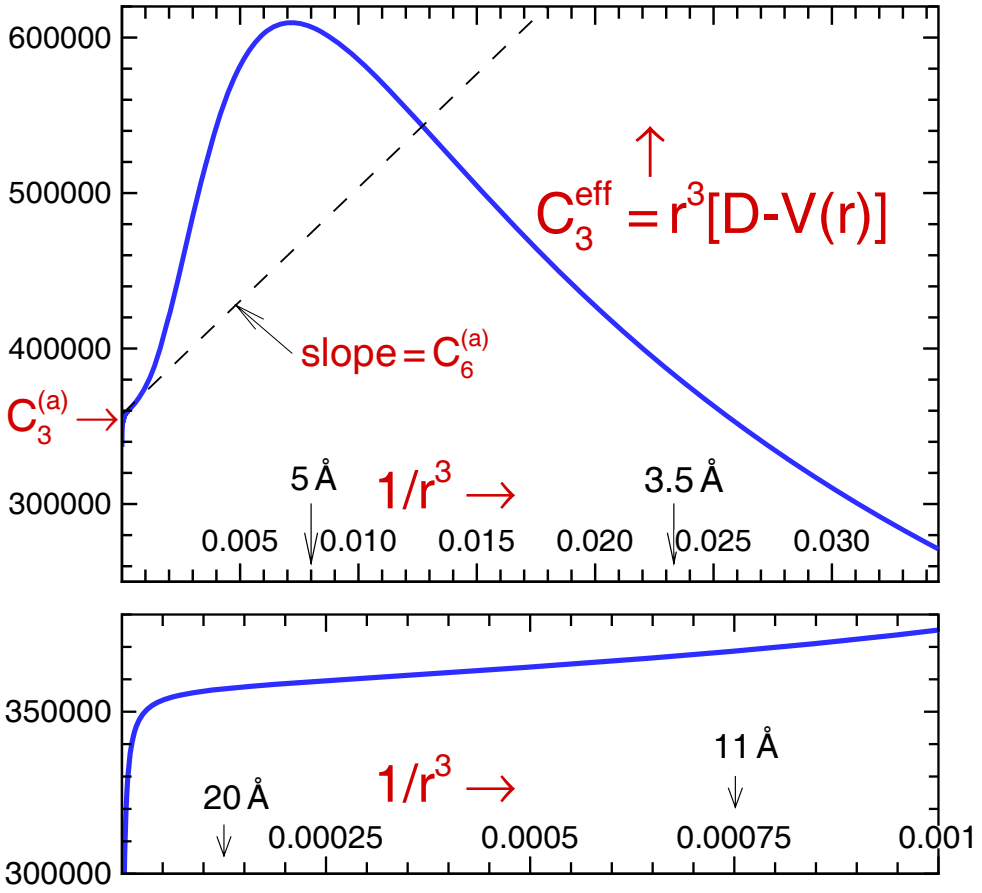

Results for $A(^1\Sigma_u^+)$ state Li_2

Analysis incomplete . . . but . . .

- good fit for $^{7,7}Li_2$ data up to $v = 92$
  [$(\mathfrak{D} - E_{v=92}) = 0.84$ cm^{-1}]
- 'limiting behaviour' plot extrapolates to $C_3^{case(a)}$ and approaches limiting slope $C_6^{case(a)}$ from above.
- *However . . .* expanding the scale in the large–r region shows a change of character!
- and at even larger r (smaller $1/r^3$) we see extrapolation to the true limiting $C_3 = C_3^{case(c)}$!

Conclusion

The generalized MLR potential function can accurately represent a potential in which spin-orbit mixing causes the long-range potential to change character!